RESEARCH ARTICLE doi.org/10.1002/adsc.202301325

Photocatalytic Oxidative Cleavage of Alkenes Followed by Carbonyl Stereoselective Bioreduction for the Synthesis of Enantioenriched Secondary Alcohols

Laura Rodríguez-Fernández,[a] Iván Lavandera,[a,*] and Vicente Gotor-Fernández[a,*]

[a] Department of Organic and Inorganic Chemistry. Instituto Universitario de Química Organometálica "Enrique Moles". Universidad de Oviedo. Avenida Julián Clavería 8, 33006, Oviedo, Spain
E-mail: lavanderaivan@uniovi.es; vicgotfer@uniovi.es

Manuscript received: November 14, 2023; Revised manuscript received: December 19, 2023;
Version of record online: January 8, 2024

Dedicated to Prof. Miquel Pericàs for his outstanding scientific career.

Supporting information for this article is available on the WWW under https://doi.org/10.1002/adsc.202301325

Abstract: Oxidative alkene cleavage of a series of (hetero)aryl alkyl styrenes in aqueous medium has been developed using either 9-mesityl-10-methylacridinium perchlorate ([AcrMes]ClO_4) and sodium anthraquinone-2-sulfonate (SAS) as photosensitizers under blue LED irradiation. Reaction conditions were studied to find a suitable media for the development of a linear cascade after subsequent stereoselective reduction of the corresponding ketone intermediate. The use of cesium carbonate provided an adequate pH to the reaction medium for the alcohol dehydrogenase action. [AcrMes]ClO_4 was found to be the best photocatalyst, allowing the development of concurrent or sequential cascades depending on the ability of the photosensitizer to oxidize back the chiral alcohol to the ketone. Overall, the photobiocatalytic approach has allowed the synthesis of a wide number of alcohol compounds, the formation of (*S*)- or (*R*)-enantiomers being attained with excellent stereoselectivity and moderate to good yields.

Keywords: Alcohol dehydrogenases; Alkenes; Cascade reactions; Oxidative cleavage; Photobiocatalysis

Introduction

Oxidative cleavage of alkenes to yield dicarbonyl compounds has been traditionally performed by ozonolysis reaction based on the *in situ* generation of ozone as terminal oxidant at very low temperatures.[1] Hazards related to the formation of ozonides and peroxides, especially during the downstream process, high waste generation, requirement of specialty equipment, and the lack of selectivity in the presence of other functional groups alert about the need for disclosing safer and sustainable olefin ozonolysis alternatives. In this context, the use of other oxidative species such as $KMnO_4$, $NaIO_4$, HIO_4, OsO_4, *tert*-butyl hydroperoxide, oxone…[2] metal-catalyzed oxidative cleavages (Co, Mn, Ru, Fe…),[2b,3] and enzymatic transformations involving non-heme and heme iron-dependent proteins,[4] provides a plethora of possibilities for the preparation of a wide number of aldehydes and ketones. From 2001, the photoinduced oxidation of α-methylstyrene using molecular oxygen in the presence of methoxybenzenes as sensitizers is known.[5] Later, the performance of photoinduced alkene oxidative cleavage reactions,[6] including metal-catalyzed (Cu, Ru, Ir…), metal-free transformations using organic dyes and enzymes is gaining increasing attention, due to the abundance of visible light in nature and the mild reaction conditions required for efficient alkene activation.

Photobiocatalysis has emerged in recent years as an elegant approach for the development of chemical transformations including the use of two green methodologies that are photo- and biocatalysis.[7] Light irradiation has allowed the activation of biocatalytic species as well as displaying a key role in the regeneration of enzymatic cofactors.[8] However, the combination of both technologies has also boosted the possibility to increase molecular complexity through the design of linear and cyclic cascades. Although, the first step can be the biotransformation followed by a photocatalytic transformation,[8] usually the preferred sequence is the generation of a reactive intermediate that is suitable for stereoselective enzyme candidates such as ene-reductases,[9] monoamine oxidases,[10] lipases,[11] transaminases,[12] and reductive aminases,[13] among others. In this context, the combination of photocatalytic methods and alcohol dehydrogenases (ADHs) is especially attractive,[14] however most of the examples have focused on the photocatalytic oxidation of alkanes, while alkene photobiochemistry has been scarcely reported. For instance, Xie and co-workers have shown the difunctionalization of styrenes through photo-oxidative fluorination and bioreduction producing chiral vicinal fluoro alcohols.[15] Herein, the synthetic potential of styrenes has been expanded to synthesize chiral alcohols on a one-pot two-step cascade approach involving their C=C bond alkene cleavage leading to the corresponding alkyl (hetero)aryl ketones (Scheme 1), which will be later stereoselectively reduced using stereocomplementary ADHs.

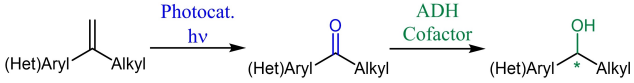

Scheme 1. Linear photobiocatalytic cascade for the one-pot conversion of alkenes into chiral alcohols.

Results and Discussion

Photocatalytic Alkene Cleavage of Methyl Styrene (1 a)

Linear cascade processes involve the conversion of an starting material into a valuable product through the formation of reactive intermediates, without the requirement of their isolation.[16] In this context, photobiocatalytic strategies have provided access to a variety of (chiral) organic molecules in a selective and straightforward manner.[17] Their successful development is threatened by two main challenges that are, the performance of individual steps with high yields and selectivities, and the search of optimal conditions to develop both transformations under a compatible operational window. For that reason, the identification of a photocatalytic oxidative system capable to produce prochiral ketones in high yields was firstly explored in the presence of water (Figure 1). Blue light was selected for the oxidative cleavage of methyl styrene (**1 a**) as model substrate, choosing water as solvent with a 10% vol of acetonitrile to assure a good solubility of the reaction mixture. Best results were found for 9-mesityl-10-methylacridinium perchlorate ([AcrMes]ClO_4) and sodium anthraquinone-2-sulfonate (SAS) leading to 95 and 98% of acetophenone (**2 a**), respectively.

SAS was selected for the optimization of the reaction conditions considering a series of parameters that affected to the ozonolysis outcome such as substrate concentration (12.5–100 mM), photocatalyst loading (2.5–7.5 mol%), organic cosolvent type (MeCN, 2-PrOH, DMSO and DMF) and percentage (2.5–10% vol), and also reaction time (2–16 h). This

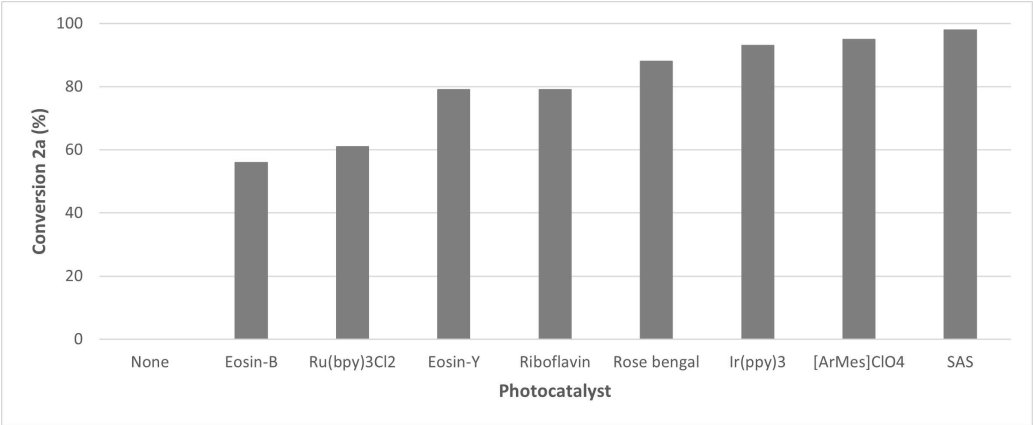

Figure 1. Photocatalyst (10 mol%) screening for the light-driven alkene cleavage of **1 a** (25 mM) under blue LED (64 W) in a MeCN:H_2O (1:9 v/v) mixture for 16 h at room temperature. See additional information in Table S1.

study is comprehensively depicted in Table S2, while the most relevant results have been summarized in Table 1. Searching for compatible conditions for the ADH action, an almost quantitative conversion was found when using **1 a** in 25 mM, a catalytic amount of the photocatalyst (5 mol%) in the presence of blue LED (64 W), a small amount of acetonitrile (2.5% vol) as cosolvent and 16 h of reaction (entry 10).

Mechanistic Studies

Control experiments were performed to demonstrate the importance of light in the formation of radical species for the oxidative cleavage of **1 a** using SAS (Table S3). For instance, the reaction did not proceed in the absence of light, discarding a thermal activation for this type of reaction. The key role of oxygen was also verified since the reaction under anaerobic conditions (argon atmosphere) proceeded in only 20% conversion towards acetophenone (**2 a**). Finally, the use of a free radical quencher, such as TEMPO, led to the complete reaction inhibition.

To study if the formation of radicals occurs through a radical propagation mechanism, switch on-off light cycles were carried out using both photosensitizers (Table S4). In both cases, continuous irradiation of blue light appeared to be necessary, as conversion values kept constant when the irradiation stopped. Finally, the presence of superoxide radical anions was also demonstrated by trapping the corresponding intermediate under aerobic conditions, which was characterized by mass spectrometry (Figures S2 and S3).

Photocatalytic Reaction Scope

Alkenes were synthesized following the procedure described by Tripathi and Mukherjee,[18] and their reactivity was highly dependent on the (hetero)aryl (R^1) and alkyl (R^2) substitutions. Under previously optimized conditions, the substrate scope was explored for alkenes **1 a**–**y** (Table 2), although in some cases the amount of SAS (entry 19) or the use of variable amounts of [AcrMes]ClO_4 (entries 9, 10, 12, 17, 23, 24 and 25) were considered to achieve more satisfactory conversions. In all cases, conversion values reached between 20 and 99%, with 10 out of 25 reactions attaining the formation of over 90% into the corresponding ketone or aldehyde.

Since all the alkenes tested possessed a terminal C–C double bond, the reaction scope was also extended to commercial (*E*)-but-2-en-2-ylbenzene (**1 z**) and (*E*)-but-1-en-1-ylbenzene (**1 aa**), satisfyingly achieving the oxidative cleavage of these internal alkenes (Figure S4). Thus, under standard reaction conditions acetophenone (**2 a**) and benzaldehyde (**2 m**) were obtained with a 90 and 95% conversion, respectively. The reactions did not show the formation of other by-products, resulting in very clean transformations.

Bioreduction Experiments

In order to adapt the first photocatalytic step to an optimal reaction medium for alcohol dehydrogenases (ADHs), different reaction media were studied to find a good relationship between conversion and a suitable

Table 1. Optimization of the reaction conditions for the light-driven alkene cleavage of **1 a** with SAS under blue LED (64 W) in aqueous medium.[a]

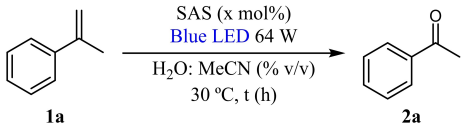

Entry	**1 a** (mM)	SAS (mol%)	MeCN (% vol)	t (h)	**2 a** (%)[b]
1	12.5	10	10	16	94
2	25	10	10	16	98
3	50	10	10	16	90
4	25	2.5	10	16	92
5	25	5	10	16	93
6	25	5	2.5	16	93
7	25	5	5	16	93
8	25	5	2.5	6	69
9	25	5	2.5	8	86
10	25	5	2.5	16	98

[a] Further information and a more comprehensive study of the reaction conditions is found in Table S2 of the Supporting Information (SI).
[b] Product percentage was calculated by GC analyses using calibration curves (see further details in the SI).

Table 2. Substrate scope for the oxidative cleavage of alkene bonds.[a]

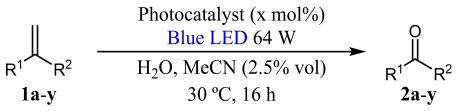

Entry	**1 a–y**	R^1	R^2	Photocatalyst[b]	**2 a–y** (%)[c]
1	**a**	Ph	Me	SAS (5)	98
2	**b**	4-OMe-C_6H_4	Me	SAS (5)	92
3	**c**	4-CF_3-C_6H_4	Me	SAS (5)	20
4	**d**	4-NO_2-C_6H_4	Me	SAS (5)	60
5	**e**	4-Cl-C_6H_4	Me	SAS (5)	76
6	**f**	4-Br-C_6H_4	Me	SAS (5)	53
7	**g**	4-F-C_6H_4	Me	SAS (5)	70
8	**h**	3-OMe-C_6H_4	Me	SAS (5)	98
9	**i**	3-Cl-C_6H_4	Me	[AcrMes]ClO_4 (5)	59
10	**j**	3-Br-C_6H_4	Me	[AcrMes]ClO_4 (5)	67
11	**k**	2-OMe-C_6H_4	Me	SAS (5)	98
12	**l**	2-Cl-C_6H_4	Me	[AcrMes]ClO_4 (5)	53
13	**m**	Ph	H	SAS (5)	>99
14	**n**	2-OMe-C_6H_4	H	SAS (5)	>99
15	**o**	2-Br-C_6H_4	H	SAS (5)	72
16	**p**	2-Naphthalene	H	SAS (5)	90
17	**q**	2-Naphthalene	Me	[AcrMes]ClO_4 (5)	40
18	**r**	3-Quinoline	Me	SAS (5)	98
19	**s**	3-Pyridine	Ph	SAS (15)	63
20	**t**	Ph	Cyclopropyl	SAS (5)	80
21	**u**	3-Pyridine	Me	SAS (5)	96
22	**v**	Ph	Et	SAS (5)	93
23	**w**	Ph	^{n}Pr	[AcrMes]ClO_4 (15)	78
24	**x**	Ph	^{n}Bu	[AcrMes]ClO_4 (10)	65
25	**y**	Ph	^{i}Pr	[AcrMes]ClO_4 (10)	40

[a] A general procedure can be found in the Experimental Section.
[b] Percentage of the photocatalysts in mol% appears in parenthesis.
[c] Product percentage was calculated by GC analyses using calibration curves (see further details in the SI).

final reaction pH for the bioreduction (Table 3). A remarkable oxidation rate into acetophenone was observed in distilled water (98%, entry 1), but the use of Tris·HCl buffers, commonly used in bioreductions, did not offer good results for the photocatalytic reaction (33–40%, entries 2 and 3). At this point, we

Table 3. Study of different reaction media in the photooxidation transformation of **1 a**.

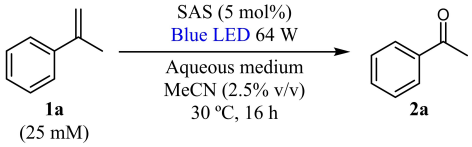

Entry	Aqueous medium	Initial pH	Final pH	**2 a** (%)[a]
1	Distilled water	5	4	98
2	Tris·HCl buffer (50 mM, pH 7.5)	7.5	6.5	33
3	Tris·HCl buffer (100 mM, pH 7.5)	7.5	7.5	40
4	Distilled water with Cs_2CO_3 (0.2 eq)	8	6	95
5	Distilled water with Cs_2CO_3 (0.25 eq)	9	7	94

[a] Product percentage was calculated by GC analyses using calibration curves (see further details in the SI).

considered adding a small amount of a weak base, such as cesium carbonate (Cs_2CO_3, 0.20–0.25 eq), to distilled water in order to maintain better the reaction pH, which resulted on the achievement of excellent conversions under conditions suitable for the ADH performance around a final neutral pH (94–95%, entries 4 and 5).

Two stereocomplementary and well-known ADHs, overexpressed in *E. coli*, namely the one from *Rhodococcus ruber* (ADH-A) and the one from *Lactobacillus brevis* (LBADH), were chosen next for the bioreduction of **2a**. Initial trials related to their reactivity are disclosed in Table S5 under magnetic stirring, finding that ADH-A behaved with excellent activity and selectivity using 0.25 eq of Cs_2CO_3 in distilled water and in the absence of light, similarly as when the use of a Tris·HCl buffer was employed.

Interestingly, both ADHs allowed the stereoselective reduction of **2a** under blue light irradiation conditions, although the process did not occur at any extension when SAS was present. The influence of the photocatalysts in the cascade process was studied incubating the racemic alcohol **3a** in the water-Cs_2CO_3 medium in presence of both photosensitizers (5 mol%, Table S6). Interestingly, the oxidation into **2a** occurred in only 8% for [AcrMes]ClO_4 after 24 h (entry 1), while with SAS the formation of acetophenone was completed (entry 2), suggesting the occurrence of a quick oxidation of the alcohol using SAS. Control experiments were carried out under optimal bioreduction conditions to study a possible inhibition of ADH-A in presence of SAS selecting ketone **2h** as substrate. Alcohol (*S*)-**3h** was obtained with excellent conversion and selectivity, when the enzyme, the photosensitizer and the substrate were added from the beginning, but also when mixing the enzyme and SAS during 16 h, and latter adding the substrate.

At this point, [AcrMes]ClO_4 was selected for the photobiocatalytic cascade design, although alcohols **3b**,**d–l**,**q**,**r**,**t**,**u**,**v**,**y**, displayed different pattern reactivity, observing the formation of the corresponding carbonyl compounds with negligible to complete conversion (Table S7).

With all these data on hand, the ADH screening of the different ketones was performed in order to find suitable enzymes for the production of the corresponding chiral alcohols, accesing to both enantiomers to properly select the ADHs (Tables S8–S15). In this context, ADH-A, ADH from *Ralstonia* species (RasADH) and ADH from *Thermoanaerobacter* species (ADH-T) demonstrated a remarkable (*S*)-selectivity, while LBADH and commercial evo.1.1.200 provided access to the opposite (*R*)-alcohol enantiomers.

Accomplishment of the Photobiocatalytic Linear Cascade

At this point, the one-pot two-step process was investigated selecting the sixteen substrate candidates **1a**,**b**,**d–j**,**l**,**q**,**r**,**t–v**,**y** that proceeded with good conversions in the oxidative alkene cleavage, also maintaining a remarkable activity and selectivity in the bioreduction processes. For alcohol substrates that were not oxidized under photocatalytic conditions into the corresponding ketones (Tables S6 and S7), a concurrent cascade methodology was developed. Thus the linear cascade was performed with five alkenes (**1a**,**d**,**q**,**r**,**u**) adding all the necessary reagents from the beginning under blue LED light irradiation (Table 4). Selecting stereocomplementary ADHs, the access to enantiopure alcohols (*S*)- and (*R*)-**3a**,**d**,**q**,**r**,**u** was possible, with values ranging from 44 to 96% depending on the ability of the photosensitizer to catalyze the oxidative alkene cleavage.

Substrates bearing phenyl and 3-quinoline rings were converted into **3a** and **3r** enantiomers (>99% *ee*) with very high conversions (88–96%, entries 1, 2, 7 and 8), while **3d**,**q**,**u** enantiomers were obtained with moderate to high yields (44–78%, entries 3–6, 9 and 10), mainly because of the recovery of significant amounts of the starting alkene (20–40%).

On the other hand, for those substrates in which [AcrMes]ClO_4 contributed to the reverse oxidation reaction of the generated alcohol, a sequential approach was envisaged (Table 5). In general excellent stereoselectivities were found when selecting the appropriate ADH, leading to the formation of 16 out of the 22 enantiopure alcohols. The alcohol percentages were highly dependent on the substitution of the aromatic ring and also to the alkyl moiety at alpha position (34–86%).

Selected scale-up experiments were performed to explore the synthetic usefulness of this approach. Thus, linear cascades with 0.6 mmol of substrate (30 mM) were run, performing the photooxidative alkene cleavage for 16 h and adding next the required reagents and the ADH for the transformation of the intermediate ketones into the corresponding alcohols **3a**,**h**,**q**,**r**,**t** (98->99% *ee*), that were recovered in 38–80% isolated yield after liquid extraction and column chromatography purification (Table 6).

Conclusions

A one-pot two step transformation of alkene derivatives into enantioenriched alcohols has been disclosed by means of the combination of photo- and biocatalytic methods. The identification of [AcrMes]ClO_4 and SAS as photosensitizers for the oxidative alkene cleavage reactions under aqueous medium, and the optimization of the conditions have allowed the production of a

Table 4. Concurrent cascade for the conversion of alkenes into enantiopure 1-(het)arylethan-1-ols.[a]

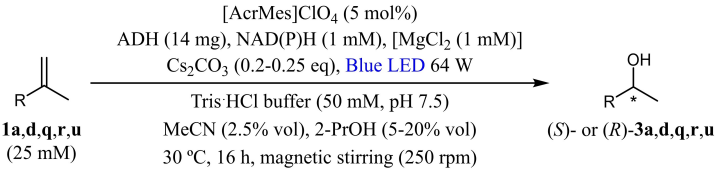

Entry	1	R	Cs_2CO_3 (eq)	2-PrOH (% vol)	ADH	1 (%)[b]	2 (%)[b]	3 (%)[b]	3 *ee* (%)[b]
1	**a**	Ph	0.20	5	*E. coli*/ADH-A[c]	4	6	90	>99 (*S*)
2	**a**	Ph	0.20	5	*E. coli*/LBADH[d]	3	4	93	>99 (*R*)
3	**d**	4-NO_2-C_6H_4	0.25	20	*E. coli*/ADH-T[e]	39	17	44	>99 (*S*)
4	**d**	4-NO_2-C_6H_4	0.25	20	evo.1.1.200[f]	22	13	65	>99 (*R*)
5	**q**	2-Naphthalene	0.20	10	*E. coli*/ADH-A[c]	40	4	56	99 (*S*)
6	**q**	2-Naphthalene	0.20	10	*E. coli*/LBADH[d]	35	10	55	>99 (*R*)
7	**r**	3-Quinoline	0.20	5	*E. coli*/ADH-A[c]	1	3	96	>99 (*S*)
8	**r**	3-Quinoline	0.20	5	evo.1.1.200[f]	<1	12	88	>99 (*R*)
9	**u**	3-Pyridine	0.20	5	*E. coli*/ADH-T[e]	29	13	68	>99 (*S*)
10	**u**	3-Pyridine	0.20	5	*E.coli*/LBADH[d]	20	2	78	>99 (*R*)

[a] A general procedure can be found in the Experimental Section.
[b] Product percentages using calibration curves and enantiomeric excess values were calculated by HPLC analyses (see further details in the SI).
[c] NADH was added.
[d] NADPH and $MgCl_2$ were added.
[e] NADPH was added.
[f] NADH and $MgCl_2$ were added.

series of (hetero)aryl alkyl ketones, which in most cases are good substrates for enzymatic carbonyl reduction. The use of a small amount of cesium carbonate provided adequate conditions for the subsequent action of the ADHs. After screening of commercial and house made enzymes, a linear photobiocatalytic cascade was accomplished using stereocomplementary carbonyl reductases.

The synthesis of a panel of alcohols was performed in a concurrent or sequential approach based on the ability of the photosensitizer to oxidize back to the ketone the generated alcohol. Thus, the substrate scope has been analyzed to provide a general methodology transforming olefins into optically active alcohols in a straightforward manner. The scalability of the sequential cascade strategy was also demonstrated using 0.6 mmol of a series of selected substrates that afforded the corresponding 1-(het)arylalkan-1-ols in moderate to good isolated yields (38–80%) and excellent optical purities (>97% *ee*).

Experimental Section

General information regarding the reagents and enzyme sources has been added in the Supporting Information. Comprehensive photocatalytic and enzymatic studies also appear in the SI, together with the full description of analytical techniques and product characterization. The authors have cited additional references within the Supporting Information.[18–34]

General Procedure for the Photocatalytic Alkene Cleavage

The corresponding alkene **1a–y** (0.075 mmol) and the photocatalyst, [AcrMes]ClO_4 (3.75–11.3 μmol, 1.54–4.62 mg) or SAS (3.75 μmol, 1.16 mg) were placed in a glass vial. Then, dry MeCN (75 μL) and distilled water (2.25 mL) were added. The vial was correctly placed in the photocatalytic set-up being irradiated with blue light under magnetic stirring for 16 h at 30 °C. Afterwards, the reaction was extracted with EtOAc (2×200 μL), transferring a sample of the organic layer (200 μL) into a GC vial and diluted with ethyl acetate (EtOAc) to a 1 mL total volume to perform GC analysis (Table 2, see further details in the SI).

General Procedure for the Concurrent Oxidative Alkene Cleavage-Bioreduction Cascade

The corresponding alkene **1a**,**d**,**q**,**r**,**u** (0.075 mmol) and [AcrMes]ClO_4 (3.75 μmol, 1.54 mg) were placed in a glass vial. Then, dry MeCN (75 μL), 2-PrOH (5–20% vol, 150–600 μL), Cs_2CO_3 (0.2–0.25 equiv., 5.3–6.1 mg) until basic pH, NAD(P)H (1 mM, 2.00 mg NADH and 2.23 mg NADPH) and 300 μL of buffer Tris·HCl (50 mM, pH 7.5) containing $MgCl_2$ (10 mM, for evo.1.1.200 and *E. coli*/LBADH) were added. Then, the volume of the vial was making up to 3 mL with distilled water. Finally, *E. coli*/ADH-A, *E. coli*-ADH-T, *E. coli*/LBADH or evo.1.1.200 were added to the reaction vial, that was correctly placed in the set-up being irradiated with blue light under magnetic stirring for 16 h at 30 °C. After this time, *tert*-butyl methyl ether (MTBE, 2 mL) was added to the vial to perform the liquid-liquid extraction. At this point, a sample containing the

Table 5. Sequential one-pot transformation for the conversion of alkyl styrenes into enantioenriched *sec*-alcohols.[a]

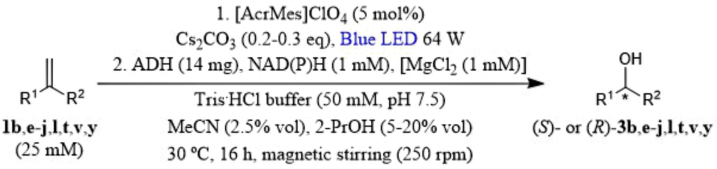

Entry	**1**	R^1	R^2	Cs_2CO_3 (eq)	2-PrOH (% vol)	ADH	**1** (%)[b]	**2** (%)[b]	**3** (%)[b]	**3** *ee* (%)[b]
1	**b**	4-OMe-C_6H_4	Me	0.20	20	*E. coli*/ADH-A[c]	9	25	66	>99 (*S*)
2	**b**	4-OMe-C_6H_4	Me	0.20	20	evo.1.1.200[d]	13	21	66	>99 (*R*)
3	**e**	4-Cl-C_6H_4	Me	0.20	10	*E. coli*/ADH-A[c]	25	11	64	>99 (*S*)
4	**e**	4-Cl-C_6H_4	Me	0.20	10	*E. coli*/LBADH[e]	20	5	75	>99 (*R*)
5	**f**	4-Br-C_6H_4	Me	0.30	20	*E. coli*/ADH-A[c]	6	8	86	>99 (*S*)
6	**f**	4-Br-C_6H_4	Me	0.30	20	evo.1.1.200[d]	8	10	82	>99 (*R*)
7	**g**	4-F-C_6H_4	Me	0.30	15	*E. coli*/ADH-A[c]	30	2	68	>99 (*S*)
8	**g**	4-F-C_6H_4	Me	0.30	10	*E. coli*/LBADH[e]	24	9	67	>99 (*R*)
9	**h**	3-OMe-C_6H_4	Me	0.25	20	*E. coli*/ADH-T[f]	20	23	57	85 (*S*)
10	**h**	3-OMe-C_6H_4	Me	0.25	20	*E. coli*/LBADH[e]	22	38	40	>99 (*S*)
11	**i**	3-Cl-C_6H_4	Me	0.25	20	*E. coli*/ADH-A[c]	34	10	56	>99 (*S*)
12	**i**	3-Cl-C_6H_4	Me	0.25	20	evo.1.1.200[d]	28	10	62	99 (*R*)
13	**j**	3-Br-C_6H_4	Me	0.25	20	*E. coli*/ADH-T[f]	30	26	44	85 (*S*)
14	**j**	3-Br-C_6H_4	Me	0.25	20	evo.1.1.200[d]	27	<1	73	>99 (*R*)
15	**l**	2-Cl-C_6H_4	Me	0.25	20	*E. coli*/ADH-T[f]	48	8	44	>99 (*S*)
16	**l**	2-Cl-C_6H_4	Me	0.25	20	evo.1.1.200[d]	44	5	51	95 (*R*)
17	**t**	Ph	Cyclopropyl	0.20	20	*E. coli*/ADH-T[f]	8	32	60	>99 (*S*)
18	**t**	Ph	Cyclopropyl	0.20	20	evo.1.1.200[d]	11	27	62	94 (*R*)
19	**v**	Ph	Et	0.30	5	*E. coli*/ADH-A[c]	<1	31	69	96 (*S*)
20	**v**	Ph	Et	0.30	5	evo.1.1.200[d]	15	12	73	96 (*R*)
21	**y**	Ph	^{i}Pr	0.20	20	*E. coli*/ADH-T[f]	56	10	34	>99 (*S*)
22	**y**	Ph	^{i}Pr	0.20	20	evo.1.1.200[d]	33	20	47	99 (*R*)

[a] A general procedure can be found in the Experimental Section.
[b] Product percentages using calibration curves and enantiomeric excess values were calculated by HPLC analyses (see further details in the SI).
[c] NADH was added.
[d] NADH and $MgCl_2$ were added.
[e] NADPH and $MgCl_2$ were added.
[f] NADPH was added.

Table 6. Scale-ups of the linear cascade experiments to transform alkenes into enantiopure *sec*-alcohols.[a]

Entry	**1**	ADH	**1** to **2** (%)[b]	**1** to **3** (%)[b]	**3** (%)[c]	**3** *ee* (%)[b]
1	**a**	ADH-A	96	84	78	>99 (*S*)
2	**a**	LBADH	93	88	80	>99 (*R*)
3	**h**	ADH-T	96	45	40	>99 (*S*)
4	**h**	LBADH	93	53	48	>99 (*R*)
5	**q**	ADH-A	58	57	50	>99 (*S*)
6	**q**	LBADH	64	54	50	98 (*R*)
7	**r**	ADH-A	85	56	53	>99 (*S*)
8	**r**	evo.1.1.200	80	53	49	>99 (*R*)
9	**t**	ADH-T	59	43	38	>99 (*S*)
10	**t**	evo.1.1.200	65	46	44	>99 (*R*)

[a] A general procedure can be found in the Experimental Section. ADH-A, LBADH and ADH-T were overexpressed in *E. coli*.
[b] Product percentages using calibration curves and enantiomeric excess values were calculated by HPLC analyses (see further details in the SI).
[c] Isolated yields after liquid-liquid extraction and column chromatography.

previously filtered organic layer (500 µL) was transferred into a HPLC vial and diluted to 1 mL total volume to perform the HPLC analysis (Table 4, see further details in the SI).

General Procedure for the Sequential Photobiocatalytic Approach

The corresponding alkene **1b**,**e–j**,**l**,**t**,**v**,**y** (0.090 mmol), [AcrMes]ClO_4 (0.0045–0.009 mmol, 1.85–3.7 mg) and dry MeCN (75 µL) were placed in a glass vial, making up its volume to 3 mL with distilled water. The reaction vial was correctly placed in the set-up being irradiated with blue light under magnetic stirring for 16 h at 30 °C. Then, 2-PrOH (5–20% vol, 150–600 µL) and Cs_2CO_3 (0.2–0.3 equiv., 5.3–8.1 mg) were added in combination with NAD(P)H (1 mM, 2.00 mg NADH and 2.23 mg NADPH) and 125–300 µL of buffer Tris·HCl (50 mM, pH 7.5) containing $MgCl_2$ (10 mM, for evo.1.1.200 and *E. coli*/LBADH). Finally, *E. coli*/ADH-A, *E. coli*-ADH-T, *E. coli*/LBADH or evo.1.1.200 were added to the reaction vial, and the reaction was left during 24 h with orbital stirring at 30 °C. After this time, MTBE (2 mL) was added to the vial to perform the liquid-liquid extraction. At this point, a sample containing the previously filtered organic layer (500 µL) was transferred into a HPLC vial and diluted to 1 mL to perform the HPLC analysis (Table 5, see further details in the SI).

General Procedure for the Scale-Up of the Sequential Photobiocatalytic Approach

Alkene **1a**,**h**,**q**,**r**,**t** (0.6 mmol, 30 mM) and [AcrMes]ClO_4 (12.4 mg, 0.03 mmol, 0.05 equiv.) were dissolved in dry MeCN (0.5 mL) and placed into a Schlenk tube. Then, the reaction volume was brought to 20 mL with distilled water. The reaction was irradiated during 16 h at 30 °C with blue LED light (64 W) under magnetic stirring. After that, 2-PrOH (5–20% vol, 1–4 mL), 2.4 mL of aqueous solution containing $MgCl_2$ (1 mM for evo.1.1.200 and *E. coli*/LBADH), NADH (1 mM for both *E. coli*/ADH-A and evo.1.1.200) or NADPH (1 mM for *E. coli*/ADH-T and *E. coli*/LBADH) and Cs_2CO_3 (0.15 mmol, 48.9 mg, 0.25 equiv.) were added. Finally, *E. coli*/ADH-A, *E. coli*/ADH-T, *E. coli*/LBADH (75 mg) or evo.1.1.200 (14 mg) was added, and the reaction was left shaking at 250 rpm for 24 h at 30 °C. The reaction crude was extracted with EtOAc (2×15 mL), combining the organic layers that were dried over anhydrous Na_2SO_4. After solvent evaporation under reduced pressure, the corresponding reaction crude was purified by column chromatography on silica gel (Hexane/EtOAc 4:1), affording the corresponding chiral alcohol in optically pure form (38–80% yield; 98- > 99% *ee*, Table 6).

Acknowledgements

Financial support from the Spanish Ministry of Science and Innovation (MCI, PID2019-109253RB-I00 and PID2022-137893OB-I00) and the Asturian Regional Government (AYUD/2021/51542) are gratefully acknowledged. L.R.-F. thanks the Asturian regional government for a predoctoral fellowship inside the Severo Ochoa programme (BP21-057). Jesús Albarrán-Velo is acknowledged for helpful discussions. The technical support of the Scientific-Technical Services of the University of Oviedo is acknowledged. We also thank Prof. Wolfgang Kroutil (University of Graz, Austria) for the donation of heterologously expressed alcohol dehydrogenases.

References

[1] a) S. G. Van Ornum, R. M. Champeau, R. Pariza, *Chem. Rev.* **2006**, *106*, 2990–3001; b) T. J. Fisher, P. H. Dussault, *Tetrahedron* **2017**, *73*, 4233–4258.
[2] a) J.-P. Wan, Y. Gao, L. Wei, *Chem. Asian J.* **2016**, *11*, 2092–2102; b) G. Urgoitia, R. SanMartin, M. T. Herrero, E. Domínguez, *ACS Catal.* **2017**, *7*, 3050–3060.
[3] P. Spannring, P. C. A. Bruijnincx, B. M. Weckhuysen, R. J. M. K. Gebbink, *Catal. Sci. Technol.* **2014**, *4*, 2182–2209.
[4] For bibliographic revisions in the field of enzymatic ozonolysis: a) F. G. Mutti, *Bioinorg. Chem. Appl.* **2012**, 626909; b) A. Rajagopalan, M. Lara, W. Kroutil, *Adv. Synth. Catal.* **2013**, *355*, 3321–3335. For recent works in this area: c) I. Hajnal, K. Faber, H. Schwab, M. Hall, K. Steiner, *Adv. Synth. Catal.* **2015**, *357*, 3309–3316; d) M. Fink, S. Trunk, M. Hall, H. Schwab, K. Steiner, *Front. Microbiol.* **2016**, *7*, 1511; e) J. Coloma, P. Hagedoorn, I. Bento, U. Hanefeld, *ACS Catal.* **2023**, *13*, 11182–11194; f) V. De Vitis, P. Cannazza, L. Mattio, D. Romano, A. Pinto, F. Molinari, T. Laurenzi, I. Eberini, M. L. Contente, *ChemBioChem* **2023**, *24*, e202300477.
[5] T. Mori, M. Takamoto, Y. Tate, J. Shinkuma, T. Wada, Y. Inoue, *Tetrahedron Lett.* **2011**, *42*, 2505–2508.
[6] R. Cauwenbergh, S. Das, *Synlett* **2022**, *33*, 129–149.
[7] a) J. Chen, Z. Guan, Y.-H. He, *Asian J. Org. Chem.* **2019**, *8*, 1775–1790; b) W. Harrison, X. Huang, H. Zhao, *Acc. Chem. Res.* **2022**, *55*, 1087–1096; c) M. A. Emmanuel, S. G. Bender, C. Bilodeau, J. M. Carceller, J. S. DeHovitz, H. Fu, Y. Liu, B. T. Nicholls, Y. Ouyang, C. G. Page, T. Qiao, F. C. Raps, D. R. Sorigue, S.-Z. Sun, J. Turek-Herman, Y. Ye, A. Rivas-Souchet, J. Cao, T. K. Hyster, *Chem. Rev.* **2023**, *123*, 5459–5520.
[8] a) J. A. Maciá-Agulló, A. Corma, H. Garcia, *Chem. Eur. J.* **2015**, *21*, 10940–10959; b) S. H. Lee, D. S. Choi, S. K. Kuk, C. B. Park, *Angew. Chem.* **2018**, *130*, 8086–8116; *Angew. Chem. Int. Ed.* **2018**, *57*, 7958–7985; c) C. J. Seel, T. Gulder, *ChemBioChem* **2019**, *20*, 1871–1897; d) S. Zhang, S. Liu, Y. Sun, S. Li, J. Shi, Z. Jiang, *Chem. Soc. Rev.* **2021**, *50*, 13449–13466; e) C.-H. Yun, J. Kim, F. Hollmann, C. B. Park, *Chem. Sci.* **2022**, *13*, 12260–12279; f) V. Alphand, W. J. H. van Berkel, V. Jurkaš, S. Kara, R. Kourist, W. Kroutil, F. Mascia, M. M. Nowaczyk, C. E. Paul, S. Schmidt, J. Spasic, P. Tamagnini, C. K. Winkler, *ChemPhotoChem* **2023**, *7*, e202200325.
[9] a) Z. C. Litman, Y. Wang, H. Zhao, J. F. Hartwig, *Nature* **2018**, *560*, 355–359; b) B. A. Sandoval, S. I. Kurtoic, M. M. Chung, K. F. Biegasiewicz, T. K. Hyster, *Angew. Chem.* **2019**, *131*, 8806–8810; *Angew. Chem. Int. Ed.* **2019**, *58*, 8714–8718; c) P. D. Clayman, T. K. Hyster, *J. Am. Chem. Soc.* **2020**, *142*, 15673–15677.

[10] a) X. Guo, Y. Okamoto, M. R. Schreier, T. R. Ward, O. S. Wenger, *Chem. Sci.* **2018**, *9*, 5052–5056; b) F. Zhao, D. Masci, S. Ferla, C. Varricchio, A. Brancale, S. Colonna, G. W. Black, N. J. Turner, D. Castagnolo, *ACS Catal.* **2020**, *10*, 6414–6421.
[11] a) Q. Yang, F. Zhao, N. Zhang, M. Liu, H. Hu, J. Zhang, S. Zhou, *Chem. Commun.* **2018**, *54*, 14065–14068; b) X. Ding, C.-L. Dong, Z. Guan, Y.-H. He, *Angew. Chem.* **2019**, *58*, 124–130; *Angew. Chem. Int. Ed.* **2019**, *58*, 118–124.
[12] J. Gacs, W. Zhang, T. Knaus, F. G. Mutti, I. W. C. E. Arends, F. Hollmann, *Catalysts* **2019**, *9*, 305.
[13] I. Peñafiel, R. A. W. Dryfe, N. J. Turner, M. F. Greaney, *ChemCatChem* **2021**, *13*, 864–867.
[14] a) K. Lauder, A. Toscani, Y. Qi, J. Lim, S. J. Charnock, K. Korah, D. Castagnolo, *Angew. Chem.* **2018**, *130*, 5905–5909; *Angew. Chem. Int. Ed.* **2018**, *57*, 5803–5807; b) W. Zhang, E. F. Fueyo, F. Hollmann, L. L. Martin, M. Pesic, R. Wardenga, M. Hohne, S. Schmidt, *Eur. J. Org. Chem.* **2019**, 80–84; c) Y. Peng, D. Li, J. Fan, W. Xu, J. Xu, H. Yu, X. Lin, Q. Wu, *Eur. J. Org. Chem.* **2020**, 821–825; d) L. Schmermund, S. Reischauer, S. Bierbaumer, C. K. Winkler, A. Diaz-Rodriguez, L. J. Edwards, S. Kara, T. Mielke, J. Cartwright, G. Grogan, B. Pieber, W. Kroutil, *Angew. Chem.* **2021**, *133*, 7041–7045; *Angew. Chem. Int. Ed.* **2021**, *60*, 6965–6969; e) F. F. Özgen, A. Jorea, L. Capaldo, R. Kourist, D. Ravelli, S. Schmidt, *ChemCatChem* **2022**, *14*, e202200855; f) Y. Zhang, H. Liu, Q. Shi, X. Chen, X. Xie, *Green Chem.* **2022**, *24*, 7889–7893; g) J. Wang, Y. Peng, J. Xu, Q. Wu, *Org. Biomol. Chem.* **2022**, *20*, 7765–7769; h) L. Rodríguez-Fernández, J. Albarrán-Velo, I. Lavandera, V. Gotor-Fernández, *Adv. Synth. Catal.* **2023**, *365*, 1883–1892.
[15] Y. Zhang, H. Liu, Q. Shi, X. Chen, X. Xie, *Green Chem.* **2022**, *24*, 7889–7893.
[16] J. H. Schrittwieser, S. Velikogne, M. Hall, W. Kroutil, *Chem. Rev.* **2018**, *118*, 270–348.
[17] a) L. Schmermund, V. Jurkaš, F. F. Özgen, G. D. Barone, H. C. Büchsenschütz, C. K. Winkler, S. Schmidt, R. Kourist, W. Kroutil, *ACS Catal.* **2019**, *9*, 4115–4144; b) F. F. Özgen, M. E. Runda, S. Schmidt, *ChemBioChem* **2021**, *22*, 790–806; c) Y. Peng, Z. Chen, J. Xu, Q. Wu, *Org. Process Res. Dev.* **2022**, *26*, 1900–1913.
[18] C. B. Tripathi, S. Mukherjee, *Angew. Chem.* **2013**, *125*, 9608–8611; *Angew. Chem. Int. Ed.* **2013**, *52*, 8450–8453.
[19] ADHs used in this work have been previously described in: *Ras*ADH: a) I. Lavandera, A. Kern, B. Ferreira-Silva, A. Glieder, S. de Wildeman, W. Kroutil, *J. Org. Chem.* **2008**, *15*, 6003–6005; ADH-A: b) K. Edegger, C. C. Gruber, T. M. Poessl, S. R. Wallner, I. Lavandera, K. Faber, F. Niehaus, J. Eck, R. Oehrlein, A. Hafner, W. Kroutil, *Chem. Commun.* **2006**, 2402–2404; ADH-T: c) Z. Findrik, D. Vasić-Rački, S. Lütz, T. Daussmann, C. Wandrey, *Biotechnol. Lett.* **2005**, *27*, 1087–1095; LBADH: d) M. Wolberg, W. Hummel, C. Wandrey, M. Müller, *Angew. Chem.* **2000**, *112*, 4476–4478; *Angew. Chem. Int. Ed.* **2000**, *39*, 4306–4308; e) J. H. Sattler, M. Fuchs, F. G. Mutti, B. Grischek, P. Engel, J. Pfeffer, J. M. Woodley, W. Kroutil, *Angew. Chem.* **2014**, *126*, 14377–14381; *Angew. Chem. Int. Ed.* **2014**, *53*, 14153–14157; *Te*SADH: f) C. Heiss, M. Laivenieks, J. G. Zeikus, R. S. Phillips, *Bioorg. Med. Chem.* **2001**, *7*, 1659–1666; HLADH: g) J. Grunwald, B. Wirz, M. P. Scollar, A. M. Klibanov, *J. Am. Chem. Soc.* **1986**, *108*, 6732–6734.
[20] J. Albarrán-Velo, V. Gotor-Fernández, I. Lavandera, *Adv. Synth. Catal.* **2021**, *363*, 4096–4108.
[21] A. Cabré, G. Sciortino, G. Ujaque, X. Verdaguer, A. Lledós, A. Riera, *Org. Lett.* **2018**, *20*, 5747–5751.
[22] T. N. Gieshoff, U. Chakraborty, M. Villa, A. Jacobi von Wangelin, *Angew. Chem.* **2017**, *129*, 3639–3643; *Angew. Chem. Int. Ed.* **2017**, *56*, 3585–3589.
[23] M. Bertolotti, E. Brenna, M. Crotti, F. G. Gatti, D. Monti, F. Parmeggiani, S. Santangelo, *ChemCatChem* **2016**, *8*, 577–583.
[24] T. T. Nguyen, L. Grigorjeva, O. Daugulis, *Angew. Chem.* **2018**, *130*, 1704–1707; *Angew. Chem. Int. Ed.* **2018**, *57*, 1688–1691.
[25] D. S. Morris, K. Van Rees, M. Curcio, M. Cokoja, F. E. Kühn, F. Duarte, J. B. Love, *Catal. Sci. Technol.* **2017**, *7*, 5644–5649.
[26] S. Zhang, D. Bedi, L. Cheng, D. K. Unruh, G. Li, M. Findlater, *J. Am. Chem. Soc.* **2020**, *142*, 8910–8917.
[27] L. Pitzer, F. Sandfort, F. Strieth-Kalthoff, F. Glorius, *Angew. Chem.* **2018**, *130*, 16219–16223; *Angew. Chem. Int. Ed.* **2018**, *57*, 16453–16457.
[28] W. Wei, X.-J. Dai, H. Wang, C. Li, X. Yang, C.-J. Li, *Chem. Sci.* **2017**, *8*, 8193–8197.
[29] D. A. Evans, F. E. Michael, J. S. Tedrow, K. R. Campos, *J. Am. Chem. Soc.* **2003**, *125*, 3534–3543.
[30] P. Song, C. Lu, Z. Fei, B. Zhao, Y. Yao, *J. Org. Chem.* **2018**, *83*, 6093–6100.
[31] A. Varenikov, G. de Ruiter, *Organometallics* **2020**, *39*, 247–257.
[32] X. Chen, Z. Lu, *Org. Lett.* **2016**, *18*, 4658–4661.
[33] S.-J. Chang, S. Zhou, H.-M. Gau, *RSC Adv.* **2015**, *5*, 9368–9373.
[34] a) K. Suga, K. Ohkubo, S. Fukuzhumi, *J. Phys. Chem.* **2003**, *107*, 4339–4346; b) Y. Zhang, X. Yue, C. Liang, J. Zhao, W. Yu, P. Zhang, *Tetrahedron Lett.* **2021**, *80*, 153321.